APD Oudoors Time-Domain Measurements for Impulsive Noise characterization

Marc Pous, Marco A. Azpúrua, Ferran Silva
Grup de Compatibilitat Electromagnètica (GCEM), Departament d'Enginyeria Electrònica (DEE)
Universitat Politècnica de Catalunya (UPC)
Barcelona, Spain
email: marc.pous@upc.edu

***Abstract*—a novel measurement and post-processing technique for estimating if impulsive noise is capable of degrading the performance of digital communication systems (DCS) is presented. It is based on the well-known capability of the amplitude probability distribution (APD) to estimate the bit-error-rate of digital communication system in the presence of electromagnetic interferences. However, the APD shall be computed from measurements taken in the absence of the useful signal of the communication system, which is a strong handicap for in-situ measurements. The main contribution of the work presented is the combination of time domain EMI measurements and decomposition techniques for separating the impulsive noise from the narrow band signals of the digital communication systems. Therefore, although the communication system signal is present at the test site, the APD diagram is obtained without the influence of the communication system, which is crucial to directly relate the shape of the diagram with the bit-error-rate introduced by the impulsive noise. This is an important step forward compared with the traditional approach as it offers the possibility to study the impact of impulsive interferences although DCS, such as broadcasting services, are present at interference scenarios.**

Keywords— Amplitude Probability Distribution, Impulsive noise, In-situ measurements, Electromagnetic interference, Electromagnetic measurements, Time-domain analysis

I. INTRODUCTION

A common type of electromagnetic interference (EMI) that is critical for current digital communication systems (DCS), is the impulsive noise or "type A" interference, defined by D. Middleton [1]. This means the noise is broadband, with bandwidths of hundreds of megahertz, and the pulses of the interferences are of short duration. A studied example of this kind of disturbance is the interference occasioned by the spark produced by the discontinuity between the pantograph and the catenary at railway applications [2], [12]. Those sparks generate impulsive noise that propagates as electromagnetic fields and, ultimately, interfere the GSM-R digital communication system. Another example is the well-known disturbance of the Digital Video Broadcasting Terrestrial (DVB-T) interfered by sources of impulsive noise like LED lamps [3].

In CISPR 16-1-1 standard, the amplitude probability distribution (APD) detector is specified for measuring electromagnetic interferences (EMI). As it has been established in several research works [4], [5], [12], this detector is suitable to crosscheck the APD measurements with the degradation that DCS suffer in terms of bit-error-rate (BER) or packet-error-rate, which are the main merit figures which are used nowadays to evaluate DCS performance. Hence, APD shall be used to characterize impulsive noise to protect communication systems, as it is required by the EMC and RED European Directives.

However, the use of APD measurements is limited due to the inconvenient that appear when traditional superheterodyne architecture instrumentation is employed to obtain the measurements. The statistical measurement shall be done at each frequency band and this causes time-limitation problematic above other limitations like being unable to apply strictly the same bandwidth as the communication system [6], [12]. Nevertheless, the novel methodologies based on time-domain captures that have recently appeared enable us to obtain fast APD results at the full frequency range [6], making feasible to implement EMI time-domain measurements in product/generic standards.

As it has been commented, another key point is to consider that many times outdoor measurements shall be carried out to ensure the compliance of a device or installation and to protect digital communication systems. For instance, to evaluate or guarantee that a fixed installation do not will produce interferences to digital communication systems such as mobile communications or broadcasting systems. These in-situ measurements have the handicap that shall be conducted in presence of the communication system that we want to protect. For instance, when in-situ measurements are done we cannot turn off broadcasting services like DVB-T, DAB or mobile communications like GSM, TETRA etc. Therefore, most of the times it is not possible to properly addressing EMC using classical measurements defined in the standards, as the communication system is masking the measurement of the EMI. In addition, this is critical when any of the detectors is employed: the QP, peak or also the new statistical ones like APD. Therefore, it is necessary to improve the outdoors in-situ measurements, as we need to be able to clearly observe the interference produced only by the impulsive noise, eliminating the contribution to the measurement of the communication system's useful signal.

Fortunately, novel full time domain measurements provide new possibilities as we have the amplitude and the phase of the measurement. Therefore, we are capable to apply post-processing techniques capable to decompose time-domain

signals/interferences [14]. In the next sections of the paper it is explained and exemplified with in-situ measurements how it is possible to obtain APD measurements, eliminating the contribution of the digital communication system present in the environment. Making possible to determine the BER that the EMI will cause to the communication system, although the signal of the communication system is present and masking the impulsive noise in the frequency domain.

II. METHODOLOGY

A. Full time domain EMI measurement

The full-time-domain EMI (Full TDEMI) measurement system employed have been developed and broadly used in recent years by GCEM-UPC [9-11]. This measurement system is based on time-domain acquisition followed by a post-processing stage, which allows obtaining equivalent results than conventional EMI test receiver. The time-domain data is acquired by a general-purpose oscilloscope and the post-processing is carried out with a standard laptop. It is important to emphasize that the time-domain capture catches the entire spectrum is measured in each acquisition, only limited by the oscilloscope bandwidth. Afterward, the amplitude spectrum of the EMI is computed applying the Short-Time Fourier Transform, non-parametric spectral estimation methods and detector emulation to deliver the results according to CISPR 16-1-1 standard. More details can be found at [9-11].

Besides computing the spectrum with the results according to the CISPR 16-1-1 standard, the time domain signal of the capture is also available. Hence, it is possible also to calculate statistical detectors likewise APD. At the following section, it is explained how to compute the APD diagram from a time domain capture obtained with the Full TDEMI measurement system.

B. APD measurement from Time domain captures

Full spectrum time-domain captures enable us to compute the APD probabilistic detector at the desired frequency band and employing the same resolution bandwidth than the actual communication channel [6], [7]. This is an advantage of using full time domain measurements instead of traditional EMI receivers according to CISPR 16-1-1. The problem is that in EMI receivers, the resolution bandwidth (RBW) of 200 kHz are not available although many communication systems such as GSM have this frequency bandwidth. The employment of the correct RBW according with the bandwidth of the DCS is particularly important when impulsive noise is evaluated. As impulsive noise is defined as a broadband disturbance, the use of filters different from the channel bandwidth of the DCS will incur in large errors. Previously, in [12] it has been demonstrated that the employment of 100 kHz or 300 kHz instead of the 200 kHz channel bandwidth in GSM receivers is traduced to an error larger than 6 dB at the APD detector output when impulsive noise is measured.

The procedure to calculate the APD from the TD captures is to down-convert the time domain signal of the frequency band that we want to evaluate at baseband and afterwards apply a low-pass filter with the same bandwidth of the communication system that we want to analyse. Upcoming, the envelope of the filtered signal is computed to finally obtain the APD diagram. APD is defined as the amount of time the measured envelope of an interfering signal exceeds a certain level [4]. The relation between the $APD_R(r)$ and the probability density function of the envelope R is

$$APD_R(r)=1-F_R(r) \tag{1}$$

and

$$f_R(r) = \frac{d}{dr}F_R(r) = -\frac{d}{dr}APD_R(r) \tag{2}$$

where $F_R(r)$ is the cumulative distribution function (cdf) and $f_R(r)$ is the probability density function (pdf). To obtain the pdf of the interference a histogram is done. Afterwards, the cdf is computed using the pdf results. Last, the APD is directly obtained from the cdf using the expressions shown above.

As it has been mentioned before, the APD main advantage compared with traditional detectors such as the QP is that it is possible to relate the APD measurement with the bit-error-probability caused by EMI. Being capable of knowing beforehand if a digital communication system will be interfered by the EMI and which is the grade of interference caused in terms of BER. Several studies have pointed a way to define limit points or limit lines at the APD diagram with the objective to clearly understand if the APD diagram of an interference will produce malfunction or not to a certain communication system [3], [4], [5], [12]. The limit points are defined considering the required bit error probability and also the sensitivity of the system. As an example that will be used later at the next section, a limit point at the APD diagram for a system that uses a QPSK modulation scheme can be calculated with the expression defined by equation (3).

$$(u_{limit}\ ,\ P_{limit}) \equiv \left(\frac{\beta_1 A}{\sqrt{m}}\ ,\ P_{req}\right) \tag{3}$$

where for a QPSK modulation scheme $\beta_1 = 1$, $m = 2$, A is the rms amplitude of the communication signal and P_{req} is the probability required by the communication system [5]. Hence, if we are available to measure the APD diagram of an impulsive noise, we can determine if it will produce an interference higher than the required BER or it will not produce a significant interference.

However, this analysis of the APD diagram with the limit line shall be done only with the contribution of the interference. If the APD diagram has also the contribution of a signal of the communication system, we will not be able to establish if the interference is harmful to the communication system. Therefore, if the interference study is done outdoors the signal of the DCS will modify the APD diagram and it will be not possible to determine if the impulsive noise will cause fault to the communication system. For this reason, at the following section, a procedure to split up the impulsive noise from the signal of the communication is explained by post-processing time domain captures.

C. Impulsive noise decomposition

The Empirical Mode Decomposition is a heuristic method developed for analyzing nonlinear and nonstationary signals. It was introduced by Huang et al. in 1998 [13]. The main capability of the EMD is to decompose complex datasets into a finite, and often small, number of components called intrinsic

mode functions (IMF) that admit well-behaved Hilbert transforms. EMD is an entirely data-driven algorithm, it does not depend on any predefined basis functions and it does not require a domain transformation.

Recently, the original empirical mode decomposition algorithm was customized in order to enhance its performance when decomposing datasets obtained from EMI measurements. Sliding window techniques allowed for processing massive acquisitions with reasonable computing resources and transient extraction capabilities enable the impulsive noise decomposition. Those techniques have been used for ambient noise cancellation applications during in-situ EMI assessments [15]. The decomposition of impulsive noise is based on the automatic time gating process that recognises pulsed events in order to separate them from the continuous wave noise. In this regard, it analyses the envelope of the EMI for estimating the instant of occurrence and the duration of the pulses. With this information, the impulsive noise can be appropriately windowed for suppressing the continuous wave components of noise outside the minor interval that comprises the impulses. Due to space constraints, it is not possible to provide a detailed description of the technique. The interested reader is suggested to consult the above-mentioned references.

III. Results / Study Case

A. Measurement Scenario

With the aim to demonstrate the capabilities of the methodology described previously, a measurement test scenario is assembled. A digital communication system signal is synthetized by an arbitrary waveform generator and propagated as an electromagnetic field by an antenna. This communication system will be switched on or off with the objective to validate the decomposition of the narrow band communication system signal and the impulsive noise. Simultaneously, a source of impulsive noise is generating a broadband interference, this interference can also be turned on or off for the validation proposes. The biconical antenna used for measuring the electric field receives at the same time the contribution from the DCS signal and the impulsive noise. In Fig. 1 a schematic of the setup is illustrated.

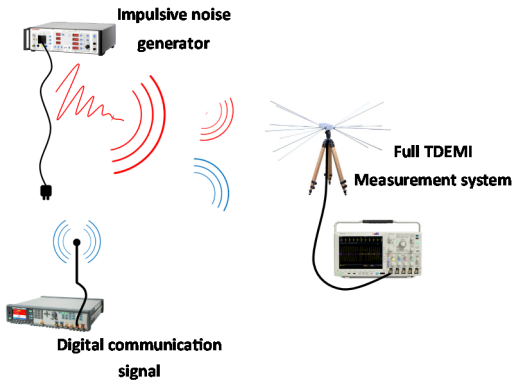

Fig. 1. Illustration of the outdoors test setup where the communication signal and the transient interference are coexisting.

Regarding the communication signal generated, it has been created by using Matlab® Simulink. A 200 kHz bandwidth QPSK signal with a square-root modulation pulse through a roll off factor of 0.2 is generated at baseband. The signal is up-converted to 40.68 MHz which is an industrial, scientific and medical (ISM) radio band and it is worldwide reserved for the use of radio frequency (RF) energy. Therefore, the synthetized signal is emulating a feasible communication system that can be encountered at any outdoor environment. The signal is delivered to the Agilent Technologies arbitrary waveform generator model 81160A, connecting its output to a biconical antenna to propagate the useful signal of the communication system. Concerning the impulsive noise, a Schölder electric fast transient generator model SFT 1400 according to EN 61000-4-4 standard is employed. The interfering pulses are coupled to a main AC wire producing disturbance electromagnetic fields. As it is defined at the standard, the rise time of the pulse is 200 ns, hence spectral components of the interference should appear at 40.68 MHz and reach the receiving measuring system.

The measuring system is composed by a PMM Biconical antenna model BC-01, which is connected to the Full TDEMI measurement system explained in section II.A. The oscilloscope (Tektronix DPO5104B) is used to capture the time domain traces and the computer is employed to control the oscilloscope, compute the frequency domain, the APD diagram and also to perform the decomposition of the signals at it has been described in section II.C.

Following different measurements are shown regarding the interference scenario. Firstly, standard APD full time-domain measurements are conducted to emphasis the necessity of eliminating the contribution of the communication system signal in order to avoid misinterpretation of the APD results.

B. Standard APD measurements results

Three different measurement are performed to highlight the differences that appear at the APD diagram. In the first measurement case only the impulsive noise is active; secondly only the signal of the DCS is present; and thirdly the impulsive interference and the DCS signal are simultaneous present.

The APD diagram is computed at the 200 kHz band centred at 40.68 MHz employing the procedure described in section II.B. In figure Fig. 2, in a blue continuous trace, it can be observed the APD diagram obtained when the DCS signal and the impulsive noise generated are active. Otherwise with a red trace it is shown the result when only the impulsive noise is present and finally, in black the APD result corresponds to the DCS signal without interference.

As it can be clearly observed from the results, the APD diagrams are overlapped when DCS is active, regardless off the impulsive noise is switched on or not. Elsewhere, when the impulsive disturbance is measured with the DCS signal turned off, the shape of the APD diagram changes to a heavy tailed distribution, which is characteristic for impulsive noise interferences. Hence, the problem of obtaining the APD diagram in presence of the DCS signal is that the useful communication signal is masking the impulsive interference.

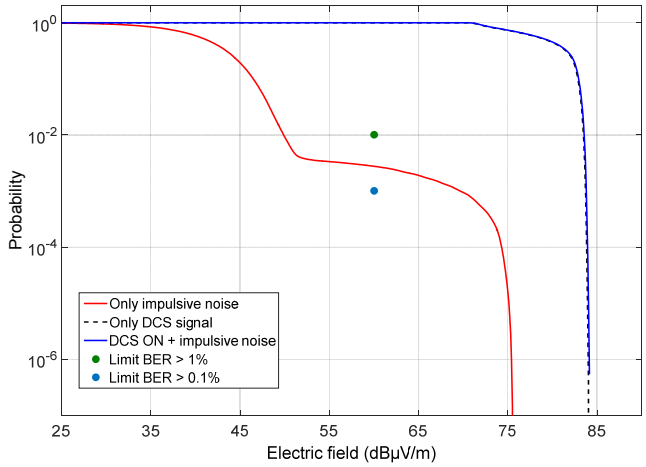

Fig. 2. APD standard measurement when the impulsive noise and the DCS signal are coexistnet, only the interference and only the DCS signal.

In Fig. 2, it can be also observed two limit points, as it has been explained before, with the APD diagram we are capable to relate the measured curve with the BER of the communication system. By means of taken into account the required BEP and the amplitude of the received signal. Related with this amplitude, it is necessary to consider that the signal of the communication system can be received with different levels. For instance, if we are evaluating a mobile DCS, the source of the communication signal is moving and the level of the received signal changes. The amplitude of the signal can be a high level but also it can be reduced according to sensitivity of the communication system. Hence, it is necessary to determine with the limits if the DCS will incur into failure due to an interference given the sensibility of the DCS or at least with an average received level. Practically, it means that even though we are receiving a level of 85 dBµV/m signal when we perform the measurement, we have to consider that the communication system can receive lower levels of useful signal in other situations to compute the limit point. In this study case, the sensibility level of the system working at 40.68 MHz is at 60 dBµV/m. Then the limit points are computed using equation (3). Where A is the rms amplitude of the communication signal and P_{req} is the probability required by the communication system. Hence, if the trace of the APD diagram is above the green point at the APD diagram, the BER will be higher than 1%, otherwise if it is above the blue point the BER will be higher than 0.1%.

If we consider the red trace in Fig. 2, which corresponds to the measurement when the DCS signal was switched off, we can determine that the impulsive interference will cause a BER between 0.1% and 1%. However, if we analyse the APD traces when the DCS signal is switched on (blue and black traces), the APD diagram contains both limit points due to the useful signal of the communication system. Making impossible to use the limit points and conclude if the communication system can be interfered by the impulsive disturbance. Unfortunately, we have to emphasize that in outdoors environments the measurement scenario will always include the signal of the communication system.

To illustrate what it is happening to the APD diagram when the DCS signal is active, the spectrum measurement of the impulsive noise generated by the fast transient generator is shown in Fig. 3. At 40.68 MHz it is observed a narrow band signal which corresponds to the DCS that has been synthetized. As the measurement has been performed outdoor other communication systems like frequency modulation (FM) broadcasting are present from 87.5 MHz to 108 MHz. Additionally, it can be also observed the broadband interference generated by the impulsive noise. The fast transient generator is causing the wide spectrum interference that can be seen from 30 MHz till above 100 MHz. Consequently, the impulsive noise is partially sharing the spectrum with the communication system at 40.68 MHz.

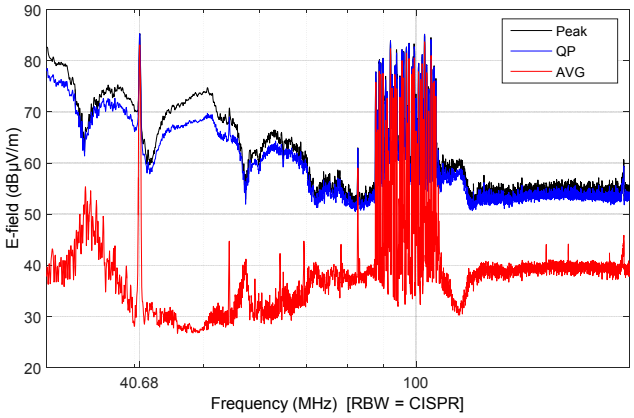

Fig. 3. Frequency domain standard measurement of the outdoor test scenario, where it can be seen the DCS signal at 40.68 MHz and the broadband impulsive noise.

Although it is clearly observed that the impulsive noise and the communication systems are sharing the spectrum, it is not feasible to unequivocally indicate if the impulsive interference will cause malfunction to the communication system from the peak, QP or average measurement.

Therefore, calculating the APD in presence of the communication signal is non-sense as the APD diagram is mostly influenced by the useful signal of the communication system. Especially as we have seen when the signal of the communication system is higher than the interference. For this reason, it is necessary to apply the decomposition method in time domain to split the impulsive noise from the communication signal.

C. Time Domain decomposition methodology to obtain APD in presence of the DCS signal

The solution proposed in this paper is to employ time domain decomposition of the measurement in order to separate the impulsive noise and calculate its APD diagram. In time domain the impulsive noise can be clearly observed and by means of decomposition time-domain techniques it can be split up from the other measured signals, which are narrow band and continuous. This opportunity of post-processing is available because in comparison with the traditional frequency sweep measurements, where we are looking only at the frequency band where we are centred, in Full time domain methodology we are observing the entire spectrum with the amplitude and

phase information. In Fig. 4, the time domain results of applying the decomposition of the interference plus the communication system obtained is observed.

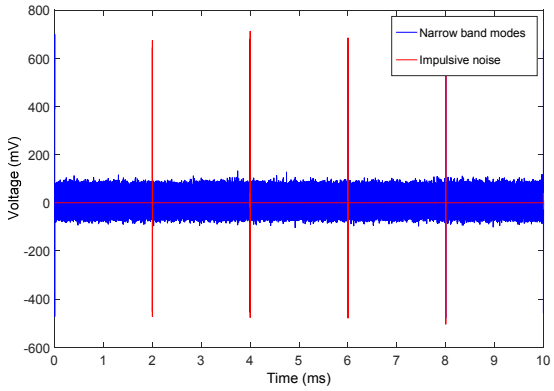

Fig. 4. Time domain decomposition applied splitting up the impulsive noise and the narrow band components.

As a characteristic of the impulsive noise, when we are observing the full spectrum, as it is done in the time-domain measurement, we can clearly identify the pulses of the broadband short duration disturbance. Therefore, it is feasible to apply the post-processing techniques and achieve the red line in Fig. 4, which is the result of splitting the impulsive noise from the narrow band signals of the communication systems.

With the aim to illustrate the accurately splitting of the impulsive noise from the narrow band signals, the frequency domain has been computed in Fig. 5. From these results, it can be verified that the decomposition of the time domain signal has been properly done.

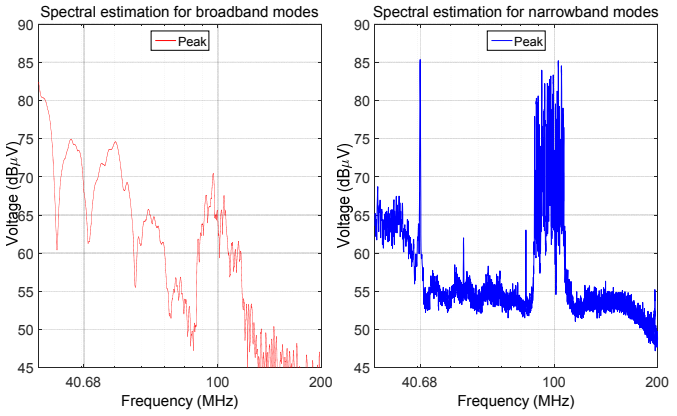

Fig. 5. Frequency domain results of the impulive noise and the narrow band DCS signals.

In Fig. 5, the impulsive noise spectrum only contains the broadband interference from 30 MHz till 120 MHz. Otherwise the spectrum produced by the narrow band modes does not include the broadband interference. Instead of, the narrow band signal from the DCS synthetized at 40.68 MHz and the FM broadcasting signal at 100 MHz is evidently identified. Therefore, it is shown that the impulsive noise has been separated properly and now we are available to compute the APD diagram considering only EMI impulsive noise.

In Fig. 6, the APD diagram of the impulsive noise obtained from the full time domain decomposition is plotted with the solid green line. For validation proposes and since it has been a scenario to demonstrate the applicability of the methodology, we have switched off the signal of the communication system working at 40.68 MHz and computed the APD diagram, which is displayed with the dashed red line in Fig. 6. Finally, the blue line is the APD diagram obtained before applying the decomposition and the influence of the useful signal is masking the entire APD result.

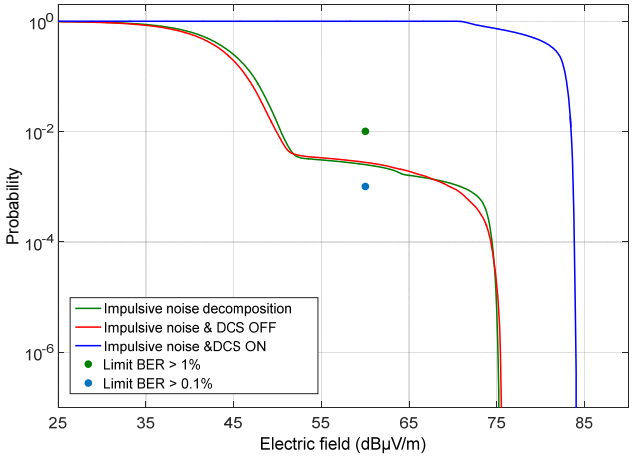

Fig. 6. APD result of the impulsive interference when the time-domain decomposition methodology is applied.

Firstly, it is important to highlight that the shape of the APD diagram is crucially changed when the signal of the communication system is eliminated. The shape is transformed from typically Gaussian noise distribution to a heavy tailed distribution, which is characteristic for impulsive noise disturbances [5], [6]. Elsewhere, the extremely good fitting between the results obtained when the decomposition method is applied with the case when the signal of the communication system is switched off demonstrate the capabilities and the benefits of the methodology developed.

Moreover, with the signal of the DCS eliminated from the APD diagram, it is possible to consider the limit points which relate the APD diagram of the EMI with its associated BER. From Fig. 6, it can be easily concluded that the BER produced by the impulsive noise will be between 0.1% and 1%. Hence, if the 40.68 MHz QPSK communication system only tolerates a BER of 0.1 % the interference will cause a failure. Otherwise we can say unequivocally that if the tolerance of the DCS is up to a BER equal to 1% the impulsive noise will not be harmful.

IV. Discussion and Conclusions

A first point of discussion is to highlight the great advantage that introduces the APD diagram, when it is combined with limit points, compared with the traditional detectors like QP which are employed at EMC harmonised standards. With the study case measurements, we have demonstrated that with the APD diagram it is possible to determine the exact BER of a

DCS when impulsive interference is disturbing the system. Once the contribution of the DCS has been removed from the APD diagram. Hence, it is essential to obtain the APD diagram without the contribution of the useful signal of the communication system, which is disgracefully always present when outdoor in-situ measurements are conducted to evaluate real interference scenarios.

In this paper, it has been demonstrated that the novel methodology combining the Full TDEMI with time-domain decomposition of impulsive noise and narrow band signals offers us the possibility to split up the impulsive noise interference from the useful DCS signal. Hence, this is the key point to be able to evaluate the possible degradation caused at the communication systems. Holding the advantage to unequivocally determine if the impulsive noise measured in presence of the communication system will cause a degradation. The methodology will conclude if the transient interference is harmful enough to cause malfunction, according to the maximum bit error probabilities tolerable and its DCS sensibility. Therefore, the novel measurement and post-processing strategy is an overwhelming opportunity for real interference scenarios where it is not available to switch off the communication system to measure and evaluate the interference. Being able to apply this methodology outdoors, especially for mobile communications where the level of the received signal is constantly changed.

ACKNOWLEDGMENT

This work was supported in part by the EURAMET 15RPT01 research project (the EMPIR is jointly funded by the EMPIR participating countries within EURAMET and the European Union) and by the Spanish "Ministerio de Economía, industria y Competitividad," under projects TEC2013- 48414-C3-3-R and TEC2016-79214-C3-2-R (AEI/FEDER, UE).

REFERENCES

[1] D. Middleton, "Canonical and quasi-canonical probability models of Class A interference,"IEEE Trans. Electromagn. Compat., vol. EMC-25, no. 2, pp. 76 103, May 1983

[2] Dudoyer, S.; Deniau, V.; Ambellouis, S.; Heddebaut, M.; Mariscotti, A., "Classification of Transient EM Noises Depending on their Effect on the Quality of GSM-R Reception," Electromagnetic Compatibility, IEEE Transactions on, vol.55, no.5, pp.867,874, Oct. 2013

[3] Wu, I.; Ohta, H.; Gotoh, K.; Ishigami, S.; Matsumoto, Y., "Characteristics of Radiation Noise from an LED Lamp and Its Effect on the BER Performance of an OFDM System for DTTB," *Electromagnetic Compatibility, IEEE Transactions on* , vol.56, no.1, pp.132-142, Feb 2014

[4] K. Wiklundh, "Relation between the amplitude probability distribution of an interfering signal and its impact on digital radio receivers," *IEEE Trans. on EMC*, Aug. 2006, pp. 537-544.

[5] Matsumoto, Y., "On the Relation Between the Amplitude Probability Distribution of Noise and Bit Error Probability," *Electromagnetic Compatibility, IEEE Transactions on* , vol.49, no.4, pp.940,941, Nov. 2007

[6] M. Pous and F. Silva, "Full-Spectrum APD Measurement of Transient Interferences in Time Domain," in *IEEE Transactions on Electromagnetic Compatibility*, vol. 56, no. 6, pp. 1352-1360, Dec. 2014.

[7] M. Pous and F. Silva, "APD radiated transient measurements produced by electric sparks employing time-domain captures," *2014 International Symposium on Electromagnetic Compatibility, Gothenburg*, 2014, pp. 813-817.

[8] M. Pous and F. Silva, "Prediction of the impact of transient disturbances in real-time digital wireless communication systems," in *IEEE Electromagnetic Compatibility Magazine*, vol. 3, no. 3, pp. 76-83, 3rd Quarter 2014.

[9] M. A. Azpúrua, M. Pous, S. Çakir, M. Çetintaş, and F. Silva, "Improving Time-Domain EMI measurements through Digital Signal Processing," *Electromagn. Compat. Mag. IEEE*, vol. 4, no. 2, pp. 66–74, 2015.

[10] M. A. Azpúrua, M. Pous, and F. Silva, "A Measurement System for Radiated Transient Electromagnetic Interference Based on General Purpose Instruments," in *Electromagnetic Compatibility (EMC EUROPE), International Symposium on*, 2015.

[11] M. A. Azpúrua, M. Pous, and F. Silva, *On the Statistical Properties of the Peak Detection for Time-Domain EMI Measurements*, vol. 57, no. 6. IEEE, 2015, pp. 1374–1381.

[12] M. Pous, M. A. Azpúrua, and F. Silva, *Measurement and Evaluation Techniques to Estimate the Degradation Produced by the Radiated Transients Interference to the GSM System*, vol. 57, no. 6. 2015, pp. 1382–1390.

[13] N. E. Huang, Z. Shen, S. R. Long, M. C. Wu, H. H. Shih, Q. Zheng, N.-C. Yen, C. C. Tung, H. H. Liu, N. E. Huang, Z. Shen, S. Long, M. Wu, H. Shih, Q. Zheng, N.-C. Yen, C. Tung, and H. Liu, "The empirical mode decomposition and the Hilbert spectrum for nonlinear and non-stationary time series analysis," Proc. R. Soc. London. Ser. A Math. Phys. Eng. Sci., vol. 454, no. 1971, pp. 903–995, 1998.

[14] M. A. Azpúrua, M. Pous and F. Silva, "Decomposition of Electromagnetic Interferences in the Time-Domain," *in IEEE Transactions on Electromagnetic Compatibility*, vol. 58, no. 2, pp. 385-392, April 2016.

[15] M. A. Azpúrua, M. Pous and F. Silva, "A single antenna ambient noise cancellation method for in-situ radiated EMI measurements in the time-domain," *2016 International Symposium on Electromagnetic Compatibility - EMC EUROPE*, Wroclaw, 2016, pp. 501-506.